



**HAL**  
open science

# Lipid oxidation in oil-in-water emulsions: Iron complexation by buffer ions and transfer on the interface as a possible mechanism

Samar Daoud, Elias Bou-Maroun, Gustav Waschatko, Philippe Cayot

## ► To cite this version:

Samar Daoud, Elias Bou-Maroun, Gustav Waschatko, Philippe Cayot. Lipid oxidation in oil-in-water emulsions: Iron complexation by buffer ions and transfer on the interface as a possible mechanism. Food Chemistry, inPress, pp.128273. 10.1016/j.foodchem.2020.128273 . hal-03013707

HAL Id: hal-03013707

<https://u-bourgogne.hal.science/hal-03013707>

Submitted on 13 Feb 2023

**HAL** is a multi-disciplinary open access archive for the deposit and dissemination of scientific research documents, whether they are published or not. The documents may come from teaching and research institutions in France or abroad, or from public or private research centers.

L'archive ouverte pluridisciplinaire **HAL**, est destinée au dépôt et à la diffusion de documents scientifiques de niveau recherche, publiés ou non, émanant des établissements d'enseignement et de recherche français ou étrangers, des laboratoires publics ou privés.



Distributed under a Creative Commons Attribution - NonCommercial | 4.0 International License

# 1 Lipid oxidation in oil-in-water emulsions: Iron complexation by buffer 2 ions and transfer on the interface as a possible mechanism

3 Samar DAOUD<sup>\*1</sup>, Elias BOU-MAROUN<sup>1</sup>, Gustav WASCHATKO<sup>2</sup>& Philippe CAYOT<sup>1</sup>

4 <sup>1</sup> Unité mixte “Procédés alimentaires et microbiologiques”. Université Bourgogne Franche-  
5 Comté, AgroSup Dijon, PAM UMR A 02.102, F-21000 Dijon, France

6 <sup>2</sup> Cargill R&D Centre Europe BVBA Havenstraat 84. B-1800 Vilvoorde, Belgium

7 \* corresponding author: Samar Daoud, E-mail: samar.daoud@u-bourgogne.fr

## 8 **Highlights**

- 9 • Iron complexation by buffer influences its ability to initiate oxidation
- 10 • The structure of buffer-iron complexes determines its reaction with oxygen
- 11 • The charge of oil-water interface modulates the lipid oxidation kinetic
- 12 • Buffer-Iron complex could migrate to the positive oil-water interface

## 13 **ABSTRACT**

14 Lipid oxidation is the main hurdle for omega-3 fatty acid enrichment in food and  
15 beverages. Fat oxidation reduces the quality and safety of supplemented products. A tuna  
16 oil-in-water emulsion (20% v/v) was exposed to iron-induced oxidation. Emulsions with  
17 changing emulsifiers and buffers were analyzed under different storage conditions (argon  
18 purging, pH variation) using Conjugated Dienes and Thiobarbituric acid reactive substances  
19 assays. The results showed that free iron ions cannot interact with oxygen. However, buffers  
20 (Citrate and phosphate) chelate iron ions (Fe (II)). Depending on the pH value and the type of  
21 buffer-Fe (II) complex, its prooxidant activity and spatial distribution are influenced. The  
22 complex charge defines the interactions with the oil-water interface, i.e., positively charged  
23 interfaces repel positively charged complexes which keeps the prooxidant away. The

24 mechanistic understanding of this work will help formulators and product developers to  
25 choose the right buffer and emulsifier combination for oxidation sensitive emulsions.

26 *Keywords*

27 Lipid oxidation

28 Oil-in-water emulsion

29 Iron-oxygen complexes

30 Iron-counter ions complexes

31 Buffer

32 Emulsifier

33 Interfacial charge

## 34 **1. Introduction**

35       Omega-3 long-chain polyunsaturated fatty acids ( $\omega$ -3 LC-PUFAs) are ranked very high  
36 in consumer awareness and health perception at all ages (Cargill, 2014). Studies showed their  
37 contribution to the development of the infant neural system (EFSA, 2014), reduction of  
38 cardiovascular disease (He, 2009), and prevention of Alzheimer (Wang et al., 2018), etc.  
39 However, the global  $\omega$ -3 LC-PUFAs intake level is low to very low in most parts of the world  
40 (Stark et al., 2016). The World Health Organization recommends higher consumption of these  
41 fatty acids (FAO/WHO, 2008). Fish and other marine foods are a great source of  $\omega$ -3  
42 LC-PUFAs. Consequently, food enrichment with fish oil is becoming a growing trend e.g.  
43 enriched milk (Let et al., 2003), etc.

44       LC-PUFAs are very prone to oxidation due to their high degree of unsaturation  
45 (Frankel, 2015). Oxidation reduces significantly product shelf-life. Lipid oxidation causes loss  
46 of nutrients, rancidity, and fishy off-flavors. Color and texture of food and beverages may be  
47 strongly impacted and even severe health issues and pathologies can be caused by lipid  
48 oxidation products (Albert et al., 2013). Aldehydes like 4-hydroxy-2-nonenal (4-HNE) and

49 4-hydroxy-2-hexenal (4-HHE) were related to adult respiratory distress syndrome, diabetes,  
50 and cancer (Liao et al., 2020; Long & Picklo, 2010).

51 In most food and beverages  $\omega$ -3 LC-PUFAs are dispersed in an aqueous phase,  
52 producing an oil-in-water emulsion. Oxidation in emulsions is known to be mechanistically  
53 more complex than in bulk oil (Laguerre et al., 2017). Trace amounts of the prooxidant ions  
54 such as iron, copper, or chrome can hardly be avoided in food production. These ions are  
55 introduced via contamination in the raw material, piping, or even is wanted for fortification as  
56 an effective and sustainable solution to iron deficiency (Martínez-Navarrete et al., 2002).  
57 Several mechanisms were proposed to describe the iron-induced lipid oxidation (Cheng & Li,  
58 2007; Schaich, 1992). The Fenton reaction (reaction of iron (II) ions  $\text{Fe}^{2+}$  with hydrogen  
59 peroxide ( $\text{H}_2\text{O}_2$ )) suggested the hydroxyl radical ( $\text{OH}^\bullet$ ) as the main inducer of lipid oxidation.  
60 A second theory proposed an optimum ratio of  $\text{Fe}^{3+}/\text{Fe}^{2+}$ , at this ratio the lipid oxidation was  
61 initiated. These theories failed to explain oxidation in some cases and were rejected by several  
62 researchers (Cheng & Li, 2007; Qian & Buettner, 1999; Yin et al., 1992). For instance, a  
63 linoleic acid emulsion with Fenton reagents could stay stable for hours when the system was  
64 separated from ambient air. Besides, when an optimum ratio (1:1) of  $\text{Fe}^{3+}/\text{Fe}^{2+}$  was applied in  
65 the same system, the oxidation rate was slower (Yin et al., 1992).

66 The impact of pH, emulsifier, particle charge and other parameters, on lipid oxidation,  
67 were studied separately or combined (Cho et al., 2003; Engelmann, 2003; Fukuzawa et al.,  
68 1988; Fukuzawa & Fujii, 1992; Mei et al., 1998; Schaich, 1992; Sørensen et al., 2008).  
69 However, the results were inconclusive. In these studies, buffers were added to emulsions  
70 (studies on lipid oxidation) or food formulations. Some authors have taken into account the  
71 metal-buffer interactions (Engelmann, 2003). Nevertheless, the majority does not indicate the  
72 buffer influence. It may result from an underestimation of the possible buffer metal

73 complexation, or non-availability of complex stability constants in the literature (Ferreira et  
74 al., 2015).

75 Citric acid is one of the most added buffers to food and beverages. It is recognized as an  
76 effective flavor enhancer. The understanding of iron-buffer interactions could help researchers  
77 and food technologists producing more chemically and physically stable emulsions. This  
78 study seeks more insights into the buffer impact on the iron prooxidant potential on lipid  
79 oxidation. Tuna oil-in-water emulsion (20% v/v oil) was chosen as a model system. Tuna oil  
80 and emulsions were characterized. Various conditions were applied. Several buffers and  
81 emulsifiers were tested. The pH level was changed. Oxidation level was measured by  
82 conjugated dienes (CD) value and thiobarbituric reactive species (TBArS) value.

## 83 **2. Materials and methods**

84 Refined tuna oil was produced and supplied by ZOR (A Cargill Company, Zaandam,  
85 The Netherlands). Oil was protected by the addition of tocopherols during production. It was  
86 purged with Nitrogen and placed in amber glass bottles at -18 °C. The list of reagents and  
87 solvents used, is provided in the supplementary data (A).

### 88 *2.1. Characterization of tuna oil*

#### 89 *2.1.1. Fatty acids (FA) composition*

90 Fatty acids composition was measured according to AOAC Method 996.06 with minor  
91 modifications (Suseno et al., 2014). Extraction and measurement were repeated three times.  
92 First, oil samples (0.18 g), Glyceryl triundecanoate (CAS Number 13552-80-2) as internal  
93 standard (0.02 g) (10% w/v), sodium hydroxide solution (0.5 M, 4 mL), isooctane (2 mL) and  
94 few boiling chips were placed in a round bottom flask. A water-cooled condenser was  
95 attached. Then, the mixture was heated under reflux for 15 min. Boron trifluoride (5 mL) and  
96 isooctane (8 mL) were added separately and heated for 5 and 1 min, respectively. Afterward,

97 the flask was left to cool for 15 min. Saturated sodium chloride solution (3 mL) was added. A  
98 small scoop of sodium sulfate was placed in a glass tube, and an aliquot of the isooctane layer  
99 was added.

100 The standard solution of FAs methyl esters (FAME) was diluted 100 times, and 10  $\mu$ L  
101 of internal standard was added. Analyses were performed using a gas chromatograph (HP  
102 6890 series, Germany) equipped with a split/split-less injector (T= 250  $^{\circ}$ C), a DB-5MS  
103 column (30m, i.d. 0.320mm, 0.5  $\mu$ m film thickness) and mass spectrometer detector  
104 5973(MS) (T=250  $^{\circ}$ C) (Agilent, USA). The carrier gas was Helium (a column flow of  
105 1.4 mL/min) and the split ratio was 100:1. The oven temperature program was as follows:  
106 11 min at 170  $^{\circ}$ C, from 170 to 200  $^{\circ}$ C at 8  $^{\circ}$ C/min (hold 1.5 min), from 200 to 210  $^{\circ}$ C at  
107 8  $^{\circ}$ C/min (hold 16 min at 210  $^{\circ}$ C), from 210 to 300  $^{\circ}$ C at 20  $^{\circ}$ C/min (hold 2 min). Finally,  
108 fatty acid percentages were determined by internal standardization without taking into account  
109 mass response factors. Calculations were performed with the integrated areas, taking into  
110 account the internal standard (Equations 1 and 2).

$$111 \quad m (FA)(g) = \frac{\text{Area (FA)} * m (S)}{\text{Area (S)}} (1)$$

$$112 \quad \% (FA) = \frac{m (FA) * 100}{m_{oil} (g)} (2)$$

113 with FA: Fatty acid and S: internal standard. The results were expressed as % of  
114 fatty acid/g (oil) (w%/w).

### 115 2.1.2. Tocopherol content

116 The method reported by Gliszczyńska-Świgło & Sikorska, 2004, was used. Oil samples  
117 (0.05–0.10 g) were dissolved in 2-propanol (1 mL). Samples were filtered (0.45  $\mu$ m filter) and  
118 transferred to 1 mL vials. Likewise, stock (100 ppm) and working solutions of tocopherols  
119 were prepared in 2-propanol. Care was taken to exclude air and light exposure for samples  
120 and standard solutions throughout the analytical procedure.

121 Analysis was performed on Shimadzu high-performance liquid chromatography (LC–  
122 20AT, Canby, OR, USA) equipped with a C18 Restek column (150mm × 4.6 mm, 5 μm). The  
123 UV-visible detector was set at 290 nm. The mobile phase was 50/50 % of  
124 acetonitrile/methanol (flow rate of 1 mL/min). The injection volume was 20 μL. Each  
125 analysis took 15 min. The α-Tocopherol peak was identified by comparing its retention time  
126 to a reference standard (retention time was 7.48 min). The concentration of α-tocopherol was  
127 estimated using an external calibration curve (0.5 to 100 ppm and  $r^2 = 0.997$ ) and expressed in  
128 mg.Kg<sup>-1</sup> of oil.

### 129 *2.1.3. Iron content*

130 Iron concentration in tuna oil was measured using the same method as Liu et al., 2019.  
131 Dry ashing method was used to destroy the organic matter. To begin, aliquots (5 g) of tuna oil  
132 were heated for more than 8 hours at 102 °C. Next, samples were transferred to the muffle  
133 furnace (500 °C) and kept for 10 hours.

134 Thereafter, each sample was dissolved in 25 mL of 2% w/w hydrochloric acid (HCl)  
135 solution. Small volumes of HCl solution were added each time and filtered (filter paper). An  
136 atomic absorption spectrometer (SpectrAA 220, Varian, Australia) was used with an  
137 air/acetylene flame. An iron lamp was set (5 mA, linearity range: 0.06 -15 ppm and  
138 248.3 nm). Furthermore, a standard curve was prepared by analyzing solutions containing  
139 known iron concentrations (0.05-1 ppm and  $r^2 = 0.996$ ). Each measurement represented an  
140 average of three acquisitions and iron content was expressed as mg.Kg<sup>-1</sup> of oil.

### 141 *2.2. Emulsion preparation and oxidation conditions*

142 Emulsions were prepared using the same process as our previous study (Daoud et al.,  
143 2019) with some slight modifications. Briefly, all emulsions were at 20% (v/v) tuna oil. The  
144 aqueous phase was buffer (70% v/v) and (10%v/v) Ferrous (II) sulfate heptahydrate  
145 (Fe (II) SO<sub>4</sub>.7 H<sub>2</sub>O) solutions. Citrate and phosphate were used as buffers (details in

146 supplementary data A). Buffers were prepared at 1 mM concentration, and pH was adjusted  
147 using hydrochloric acid (HCl) or sodium hydroxide (NaOH) solutions. Iron solution (1 mM)  
148 was added to the aqueous phase (final concentration in emulsions 0.1 mM). Subsequently,  
149 emulsifiers at the concentration of 1% (w/v) for Hexadecyltrimethylammonium bromide  
150 (CTAB) and sodium dodecyl sulfate (SDS), and 3.7% (w/v) for Tween20 were used to  
151 produce the emulsions. Tuna oil and aqueous phase were blended three times (1 min each  
152 time) at 20,500 rpm using a rotor/stator homogenizer (Ultra Turrax® T25; IKA-Labortechnik,  
153 Munich, Germany). The coarse emulsion was then homogenized four times at 35 MPa using a  
154 microfluidizer (LM10; Microfluidics, Westwood, MA, USA).

155 Finally, each preparation was distributed into three vials: 10 mL of each sample were  
156 placed in 30 mL vial. In contrast, for the experiment with argon purging, smaller vials (2 mL)  
157 were used. The empty vials were purged for 20 seconds prior to the addition of samples.  
158 After, emulsions (1 mL) were placed inside and purged for 40 seconds with 5 mL/min flux.  
159 These conditions were set to ensure total removal of oxygen dissolved in the emulsion and  
160 present in the headspace. Samples were kept in dark at 30°C for 30 days.

### 161 2.3. *Characterization of oil in water emulsion*

#### 162 2.3.1. *Particle size*

163 The oil droplet size was measured by a Mastersizer 2000 (Malvern Instruments Co.,  
164 Ltd., Worcestershire, UK). The emulsion was dispersed in the corresponding buffer to fit the  
165 obscuration range (0-12%). The refractive indexes of oil and dispersant (water) were set  
166 at 1.48 and 1.33, respectively. The mean of five scans was calculated for each measurement.  
167 Moreover, measurements were repeated on three replicates. Data were then analyzed by  
168 Mastersizer 3000 software. The particle size distribution was determined by the application of  
169 the Mie theory. Then, the volume-surface average diameter ( $d_{3,2}$ ) and volume average



170 diameter ( $d_{4.3}$ ) were expressed in  $\mu\text{m}$  as the mean values of three replicates  $\pm$  standard  
171 deviation.

### 172 2.3.2. Particle charge

173 The oil droplet charge was evaluated by measuring the zeta-potential (mV). A zetameter  
174 CAD Zetacompact® (CAD Instrument, Les Essarts Le Roi, France) was used to measure  
175 these two parameters. To start, emulsions were greatly diluted in the corresponding buffer  
176 solution until a sparser particle distribution. The measurements were carried out at room  
177 temperature. Data were presented as an average of three repetitions (separate injections).

### 178 2.4. Iron-buffer interaction by UV spectroscopy

179 Solutions of iron at 0.1 mM and buffers (citrate and phosphate) at 1 mM were prepared.  
180 These concentrations were selected to mimic those of prepared emulsions. The UV spectra of  
181 these solutions as well as solutions of iron and buffers separately were recorded. Also,  
182 solutions of citrate buffer and iron were prepared at different pH values (2.5, 3.9, 5.6, and  
183 7.2). Each sample was measured using a UV-Vis spectrophotometer (UVmc ®, SAFAS,  
184 Monaco) with a data interval of 1 nm and a band path of 2 nm. Spectra were recorded in the  
185 range of 200 to 800 nm.

### 186 2.5. Evaluation of the oxidation level

#### 187 2.5.1. Determination of the CD value

188 Before analysis, the fat part was extracted (Daoud et al., 2019). Mixture of  
189 isooctane/2-propanol (3:1) (1 mL) and sodium chloride (0.024 g) were added to 0.2 mL of  
190 emulsion. The mixture was vortexed for 1 min and left to stand for 1 min for phase separation.  
191 Afterward, the upper layer (20-50  $\mu\text{L}$ ) was diluted in isooctane. Absorbance spectra were  
192 recorded between 200 and 300 nm using a UV-VIS spectrophotometer (UVmc ®, SAFAS,  
193 Monaco) with a data interval of 1 nm and a band path of 2 nm. Pure isooctane was used as a

194 reference. The value of CDs was expressed in millimoles of equivalents peroxide per  
195 kilogram of oil ( $\text{mmol eq peroxide}\cdot\text{kg}^{-1}_{\text{oil}}$ ) using a molar extinction coefficient of  
196  $27000 \text{ M}^{-1}\cdot\text{cm}^{-1}$  at 233 nm.

### 197 *2.5.2. Determination of TBArS value*

198 TBArS value was determined according to the original method described by (McDonald  
199 & Hultin, 1987). Briefly, TBA reagent was prepared by mixing 0.375 g of thiobarbituric acid  
200 (TBA), 15 g of trichloroacetic acid (TCA), 1.76 mL of HCl, and 98.24 mL of water. To avoid  
201 further oxidation, 3 mL of a 2% solution of Butylated hydroxytoluene (BHT) in Ethanol was  
202 added to 100 mL of TBA reagent. Then, 100  $\mu\text{L}$  of emulsion, 400  $\mu\text{L}$  of water, and 1 mL of  
203 TBA reagent were mixed in Eppendorf tube (2 mL capacity). Samples were placed in a water  
204 bath ( $100\text{ }^{\circ}\text{C}$  for 15 min). Samples were left to cool down for 3 min before centrifuging  
205 for 1 min at 10000 rpm using Eppendorf® Microcentrifuge 5415D (Eppendorf AG,  
206 Barkhausenweg, Hamburg, Germany). Once the upper layer was transferred directly or  
207 diluted to the cuvette, the UV-spectra were recorded in the range of 500 to 600 nm using the  
208 UV-Vis spectrophotometer (UVmc ®, SAFAS, Monaco). The data interval was set at 1 nm  
209 and the band path at 2 nm. The concentration of aldehydes was calculated using the standard  
210 curve. The standard curve was prepared with tetramethoxypropane (TMP): eight standards,  
211 ranging from 0 to 30  $\mu\text{M}$  and  $r^2 = 0.999$ . TBArS value was expressed in millimolars of  
212 equivalents malondialdehyde per liter of emulsion ( $\text{mM eq MDA}\cdot\text{L}^{-1}$  of emulsion).

### 213 *2.6. Statistical tests*

214 To assess significant differences, analysis of variance (one-way ANOVA) followed by  
215 means comparison using the Tukey test was applied. The level of significance was set to 95%  
216 ( $p = 0.05$ ). Statistical tests were performed using the Minitab® (version 18.1; PA, USA).

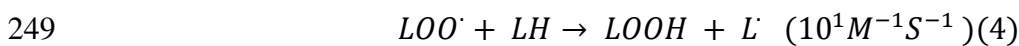
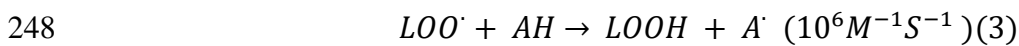
### 217 **3. Results and discussion**

#### 218 *3.1. Preliminary test: defining the major parameters of lipid oxidation*

219 Emulsion with 1 mM citrate buffer at pH 7 and iron solution (0.1 mM) was prepared  
220 and placed in 2 mL vials (ratio emulsion to the headspace of 1 (v/v)). The oxidation level was  
221 evaluated by CD values. A lag phase of 5 days was noticed (Figure 1). CD value increased  
222 after attaining a maximum of 112 mmol eq peroxide.Kg<sup>-1</sup> oil and then decreased. This  
223 phenomenon is frequently observed with CD or peroxide value records. The primary product  
224 content increases with the degree of oxidation and reaches a maximum. Afterward, the  
225 primary products (peroxides) are transformed in secondary products which results in a  
226 decrease in their concentration.

227 Fish oil was used in this study because of its low oxidative stability. Its FA composition  
228 confirmed it (Table 1). The repartition of fatty acids was in good compliance with the codex  
229 of fish oils (Codex Alimentarius Commission, FAO, WHO, 2017), and other researchers'  
230 works (Nazir et al., 2017; Suseno et al., 2014). In general, the tuna oil was dominated by  
231 palmitic acid (C 16:0) (19.5 %wt.) as the major saturated fatty acids (SFAs) and oleic acid  
232 (C18:1) (18.8 %wt.) as the main monounsaturated fatty acids (MUFAs). As for  
233 polyunsaturated fatty acids (PUFAs), eicosapentaenoic acid (EPA) (8.9 %wt.) and  
234 docosahexaenoic acid (DHA) (25.3 %wt.) were the most abundant. The total PUFAs in tuna  
235 oil reached 41.2 %wt. It is well known that the ability to be oxidized could be linearly related  
236 to the number of bis-allylic positions present in the fatty esters (two times higher for every  
237 active bis-allylic methylene group) (Frankel, 2015). In addition, the decomposition of  
238 hydroperoxides starts earlier in the presence of a high amount of PUFA, which confirms the  
239 rapid drop of the CD values (Figure 1a). Besides, the initial iron content in tuna oil was  
240 estimated as  $0.71 \pm 0.35$  mg.Kg<sup>-1</sup> of oil (Table 1). Iron content in fish oil should be within the  
241 range of 0.5 to 7 mg.Kg<sup>-1</sup> for crude oil and  $\leq 1.5$  mg.Kg<sup>-1</sup> for refined fish oil (Hoan & Son,

242 2018). However, the lag phase was seen because tuna oil was enriched with tocopherol  
243 (vitamin E). The  $\alpha$ -Tocopherol content in oil used in this study was about  $1282 \text{ mg.Kg}^{-1}_{\text{oil}}$   
244 (Table 1). A maximum amount of  $6000 \text{ mg.Kg}^{-1}$  of  $\alpha$ -Tocopherol or mixture can be added to  
245 preserve fish oil (Codex Alimentarius Commission, FAO, WHO, 2017).  $\alpha$ -Tocopherol (AH)  
246 reacts rapidly with peroxy radicals ( $\text{LOO}\cdot$ )(Equation 3). This reaction is faster than the  
247 reaction of peroxy radicals with other lipid molecules (LH) (Equation 4).



250 By hydrogen atom donation, lipid hydroperoxides (LOOH) and tocopherol radical ( $\text{A}\cdot$ ) are  
251 produced. Tocopherol radical is stable by resonance thus, the radical chain reaction does not  
252 propagate (Frankel, 2015).

253         Afterward, the same experiment was repeated but emulsion was purged with argon.  
254 Flushing emulsion with argon provided an inert atmosphere. Hence, conjugated dienes values  
255 of these samples remained permanently low during several weeks (Figure 1). Regardless of  
256 some fluctuations, no significant changes were observed over the storage period (one-way  
257 ANOVA  $p < 0.05$ ) (supplementary data (B)). Identical results were obtained for emulsions  
258 with phosphate buffer (10 mM) and iron (0.01 mM). Nitrogen and argon-purged emulsions  
259 remained stable over 30 days of storage (supplementary data (B)). The unique presence of  
260 iron is insufficient for initiating lipid radicalization. Consequently, complete hypoxia is a  
261 great way to preserve fragile oil against oxidation (Yin et al., 1992).

262         A positively charged emulsifier (CTAB) was used with the preconception that  
263 positively charged ferric ions cannot reach a positively charged interface. However, the iron  
264 ions ( $\text{Fe}^{2+} / \text{Fe}^{3+}$ ), in the presence of oxygen, were able to reach the interface. Hypervalent  
265 iron-oxygen complexes such as ferryl (IV) ( $\text{FeO}^{2+}$ ), perferryl (V) ( $\text{FeO}^{3+}$ ), or mixed iron  
266 oxygen complexes ( $\text{Fe}^{2+}\text{-O}_2\text{-Fe}^{3+}$ ) were mentioned as responsible for lipid oxidation (Cheng

267 & Li, 2007; Lee et al., 2010; Qian & Buettner, 1999; Schaich, 1992). These species have a  
268 high redox potential and are stereospecific oxidants in H-abstraction. The dioxygen (triplet  
269 state) cannot react directly with iron (singlet state), because of spin restriction. Nevertheless,  
270 iron chelation induces a significant energy rearrangement to “3d” or “4s” orbitals, resulting in  
271 the removal of the spin barrier (Yin et al., 1992). In this experiment, chelators were not added.  
272 Some authors mentioned the potential of buffers (phosphate, citrate...) to compete with iron  
273 chelators (Ferreira et al., 2015; Yin et al., 1992). Could buffers chelate iron and help its  
274 interaction with oxygen? What is the reactivity of buffer-iron-oxygen complexes?

### 275 *3.2. Buffer role in lipid oxidation*

276 A new set of samples was prepared with iron solution at 0.1 mM. Two buffers were  
277 tested: citrate and phosphate. The pH was set at 7 (buffer at 1 mM). The oxidation level was  
278 monitored using the CD value.

279 CD values increased rapidly from approx. 50 to 250 mmol eq peroxide.Kg<sup>-1</sup> oil  
280 (Figure 2a). It was noticed that the buffer type impacted on lipid oxidation. Only after three  
281 days, the CD values of these two emulsions were significantly different (one-way ANOVA  
282 based on buffer's type; p<0.05). Moreover, the induction time was determined by the time  
283 when the CD value was significantly different than the day before (one-way ANOVA with the  
284 time factor, supplementary data (C)). Induction times were between seven to ten days for  
285 citrate and four days for phosphate (designated by arrows in Figure 2a). Thus, the emulsion  
286 with citrate buffer was the most stable.

287 Besides, iron complexation by buffers changes according to the pKa and pH values  
288 (Kristinova et al., 2014). As shown in Figure 2b, citric acid has three values of pKa (3.13,  
289 4.76, and 6.4) and phosphate has also three (2.15, 7.2, and 12.33). At pH 7, the citrate (Cit<sup>3-</sup>)  
290 is in majority in comparison of monohydrogenocitrate:

291 
$$pH = pKa + \log \frac{Base}{acid} = pKa + \log \frac{[Cit^{3-}]}{[CitH^{2-}]} \quad (5)$$

292 
$$\frac{[Cit^{3-}]}{[CitH^{2-}]} = 10^{(pH-pKa)} = 10^{(7-6.4)} = 3.98 \quad (6)$$

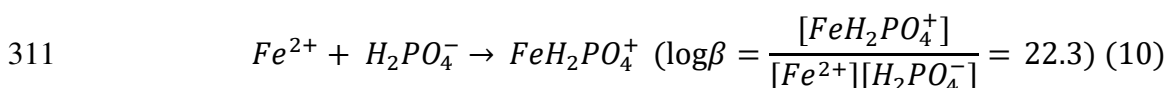
293 The percentage of  $Cit^{3-}$  of the total citrate ( $Cit^{3-} + CitH^{2-}$ ) can be estimated as follow:

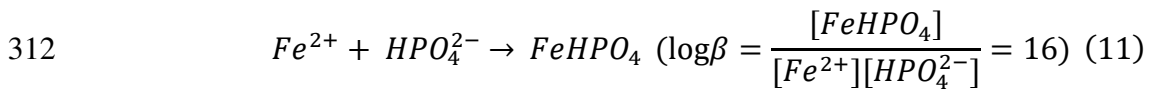
294 
$$\frac{[Cit^{3-}]}{[Cit^{3-}] + [CitH^{2-}]} = \frac{3.98 [CitH^{2-}]}{3.98 [CitH^{2-}] + [CitH^{2-}]} = \frac{3.98}{1 + 3.98} = 0.799 \quad (7)$$

295 The totality of citric acid is charged: approximately 80% is totally deprotonated ( $Cit^{3-}$ )  
 296 and the rest is monohydrogenocitrate ( $CitH^{2-}$ ). Following the same strategy (Equations 5, 6,  
 297 and 7), the distribution of phosphate species can be defined. At pH 7, phosphate is mainly  
 298 presented as dihydrogenophosphate  $H_2PO_4^-$  (61%), and monohydrogenophosphate  $HPO_4^{2-}$   
 299 (39%). All of these species are negatively charged and can play the role of counter-ion (iron  
 300 ions or hypervalent iron-oxygen complexes).

301 Citrate and phosphate can complex iron (Cho et al., 2003; Ferreira et al., 2015; Yin et  
 302 al., 1992). These complexes can be detected at 250 and 275 nm after the addition of iron to  
 303 citrate and phosphate solutions, respectively (supplementary data (C)). The peaks were also  
 304 mentioned in other studies (Francis & Dodge, 1993; Königsberger et al., 2000; Seraghni et al.,  
 305 2012; Yin et al., 1992).

306 The complexation of ferrous ions with citrate and phosphate buffers as the constants of  
 307 complexation ( $\log\beta$ ) is presented in reactions (8 and 9) and (10 and 11), respectively  
 308 (Königsberger et al., 2000; Mao et al., 2011).





313 Phosphate buffer had higher values of stability constants ( $\log\beta$ ). The resulting  
314 complexes are mainly positively charged ( $FeH_2PO_4^+$ ) (reactions 10 and 11). In contrast, the  
315 majority of iron (II) -citrate complex is negatively charged ( $FeCit^-$ ). Can iron complexation by  
316 buffer impact its position in the emulsion? Can iron-citrate complex migrate towards the  
317 positively charged interface?

### 318 *3.3. Impact of buffer on iron location and activity in the emulsion*

319 Emulsions were prepared with citrate buffer (1 mM), CTAB as an emulsifier, and  
320 iron (II) solution at 0.1 mM. Four pH levels were tested: 2.5, 3.9, 5.6, and 7.2. All samples  
321 were kept in dark at 30 °C.

322 First, the particle size was measured. The values of  $d_{3,2}$  ranged from 0.53 to 0.57  $\mu m$  and  
323  $d_{4,3}$  from 0.56 to 0.62  $\mu m$ . At pH 7.2, droplets were slightly bigger. But no significant changes  
324 were seen regarding the pH (one-way ANOVA analysis  $p < 0.05$ , applied on  $d_{4,3}$  and  $d_{3,2}$   
325 values) (details in supplementary data (D)). All emulsions were stable: no coalescence or  
326 flocculation was observed over the storage period. The particle charge was evaluated by the  
327 variations of mobility ( $\mu m/s/V/cm$ ) and zeta-potential (mV) (supplementary data (D)). CTAB  
328 is always positively charged: it is permanent quaternary ammonium ( $R_1R_2R_3R_4N^+$ ) and the pH  
329 does not influence its charge (no proton exchange). However, when the pH of emulsions  
330 increased, the zeta-potential decreased from 43 to 14 mV, then flipped to negative values of --  
331 15 and -30 mV (Figure 3a). At different pH, several species of citrate are present in the  
332 solutions (Figure 3a). For instance, at pH 2.5 citrate is mainly protonated (81% of acid,  $H_3Cit$ ,  
333 and 19% of the conjugated base  $H_2Cit^-$ ). Complexation of iron by citrate is low. Citrate cannot  
334 transfer iron ions, the interface charge remained positive. When the pH increase, citrate is  
335 gradually deprotonated. It is more available to complex iron ions and conveys it to the

336 interface. Iron-Citrate complex changes the apparent charge at the interface. In general, the  
337 zeta-potential is a great representation of the electrical characteristics of an emulsion droplet  
338 because it inherently accounts for the adsorption of any charged counter-ions (Cano-  
339 Sarmiento et al., 2018). The charge of iron-citrate complexes varies from positive to more  
340 negative with increasing pH. This phenomenon was also mentioned in other studies  
341 (Fukuzawa, 2008).

342 At a higher level of pH, iron complexation by citrate becomes more important. It was  
343 proved by the UV-spectra of the iron-citrate solutions (at different pH) (Figure 3b). The  
344 spectra of iron and citrate solutions alone were reduced from the solutions spectra. When the  
345 pH increase, the peak of the iron-citrate complex near 250 nm increased. Citrate comprised  
346 more possible sites to complex iron. The resulting complex migrates to the interface and  
347 amends its absolute charge. The state of emulsion interface and the possible migration of  
348 iron-oxygen-buffer complexes are schematized in Figure 3a.

349 Iron complexation by citrate facilitates its migration near the interface (CTAB as an  
350 emulsifier). However, when citrate was used as a buffer the emulsion was more stable to  
351 oxidation. Complexation affinity cannot explain alone the difference in the oxidation levels of  
352 the two prepared emulsions. When iron complexation was considered retarding lipid  
353 oxidation, in several cases, it was the opposite. For instance, the stability constants of  
354 diethylenetriaminepentaacetic acid (DTPA) and ethylenediaminetetraacetic acid (EDTA) with  
355 iron (II) ions are very similar. Their addition led to different oxidation rates in  
356 iron (II)-linoleic acid emulsion (Yin et al., 1992). The reaction of complexed-Fe (II) with  
357 oxygen is mainly controlled by the structure of this complex. To be able to react with oxygen,  
358 complexed-iron should still present at least one free site or occupied by a labile water  
359 molecule. When reaction with oxygen is possible, the Fe (II) autoxidation can occur



360 (production of Fe (III) -complex), Fe (II) -complex-O<sub>2</sub> is no more present to accelerate lipid  
361 oxidation.

362 In the presence of citrate, nuclear magnetic studies confirmed that the ferrous citrate  
363 complex (FeCit<sup>-</sup>) is tridentate. Fe (II) is involved with two carboxylic acid groups and the  
364 hydroxyl group of citrate and the fourth bond is with a water molecule (Francis & Dodge,  
365 1993). This structure eases the autoxidation of the ferrous citrate complex. This fast  
366 autoxidation retards the initiation of lipid oxidation. Other studies conferred about the  
367 presence of a dimeric iron citrate complex (FeCit<sub>2</sub><sup>4-</sup>) at pH 7 ( $\log\beta = 7$ ). The formation of this  
368 dimeric complex also increased the iron (II) oxidation rate: in the presence of citrate (ratio of  
369 1:10 (iron: citrate)) oxidation rate was at least two times higher (Pham & Waite, 2008).

370 A speciation study on Fe (II) autoxidation kinetics in the presence of phosphate, showed  
371 that FeH<sub>2</sub>PO<sub>4</sub><sup>+</sup> and FeHPO<sub>4</sub> are the two major phosphates complexes at pH 6.5-7.5 (Mao et  
372 al., 2011). Both complexes do not promote iron autoxidation. As a result, these phosphate-  
373 iron complexes are more available to initiate lipid oxidation. These findings comply with the  
374 oxidative stability seen higher for emulsion with citrate buffer compared to phosphate buffer.  
375 Since the structure and charge of resulting complexes are important, the interface charge has  
376 also a role in lipid oxidation.

### 377 *3.4. Impact of interface charge on lipid oxidation*

378 Three emulsions were prepared at both pH 2.5 and 7.2. The same buffer and iron  
379 concentrations were maintained. Three emulsifiers were tested: CTAB (positively charged),  
380 Tween20 (no charge), and SDS (negatively charged).

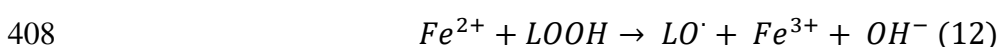
381 The particle size of emulsions with SDS and Tween20 were in the same range of  
382 emulsions with CTAB emulsifier. Emulsions stabilized with SDS had d<sub>4:3</sub> of  
383  $0.569 \pm 0.008 \mu\text{m}$  and d<sub>3:2</sub> of  $0.538 \pm 0.006 \mu\text{m}$ . Emulsions with Tween20 emulsifier also  
384 presented lower values of d<sub>4:3</sub> ( $0.528 \pm 0.001 \mu\text{m}$ ) and d<sub>3:2</sub> ( $0.5 \pm 0.001 \mu\text{m}$ ). The zeta

385 potential values were  $7.69 \pm 1$  and  $3.09 \pm 7.2$  mV respectively for SDS and Tween20  
386 stabilized emulsions. The zeta potential of the emulsions prepared with Tween 20 and SDS  
387 was less important compared to emulsion prepared with CTAB emulsifier.

388 At pH 2.5, there was no significant difference in the CD values (test of equal variance  
389  $p < 0.05$ ) (supplementary data (E)). In contrast, the TBARS test presented some significant  
390 variations (Figure 4a). At pH 2.5, emulsions with CTAB emulsifier revealed no changes in  
391 TBARS values through the storage time (test for equal variance  $p < 0.05$ ). The TBARS of  
392 emulsion with SDS was significantly increasing since the first day. A similar phenomenon  
393 was identified for emulsion with a neutral interface (Tween20) but with a lower extent.

394 At pH 7.2, the citrate (86%  $\text{Cit}^{3-}$ ) is in majority in comparison of monohydrogenocitrate  
395 (14 %  $\text{CitH}^{2-}$ ) (ions distribution obtained by equations 5, 6 and 7, with  $\text{pH} = 7.2$  and  $\text{pKa} =$   
396 6.4). The neutral Tween20 emulsifier presented the most stable emulsion (slight variations  
397 seen with one-way ANOVA  $p < 0.05$ ). The CD values were lower than those with CTAB and  
398 SDS emulsifiers. Once again SDS emulsion was the less stable (supplementary data (E)). As  
399 for TBARS values, the same order as at pH 2.5 was noticed, SDS stabilized emulsion was the  
400 less stable emulsion followed by Tween20 and CTAB emulsion (Figure 4b).

401 Compared to SDS and Tween20, CTAB-emulsion was more stable. TBARS values at  
402 pH 2.5 and 7.2 were almost stable during the storage time (Figure 4). The positively charged  
403 interface repelled iron ions and retarded the oxidation. SDS negatively charged interface  
404 attracted iron and iron-oxygen ions. Hence, iron was closer to the peroxides molecules  
405 (LOOH) (present near the interface due to their hydrophilic head). Iron ions decomposed  
406 peroxides to form alkoxy ( $\text{LO}^\bullet$ ) radicals (Equation 12). These interactions accelerated the  
407 lipid oxidation rate.



409 For instance, at pH 2.5, the initial TBARS value of SDS-emulsion was 12 and 26 times  
410 higher than Tween20 and CTAB emulsions. As for Tween20 emulsion, iron ions could still  
411 approach the interface through ion-dipole interactions. However, these interactions are weaker  
412 than ion-ion interactions (Mei et al., 1998; Schaich, 1992).

413 Moreover, the important oxidation in negatively charged emulsion could be associated  
414 with the rapid tocopherol oxidation in such emulsion. Iron ions (attracted by the interface) can  
415 interact with tocopherol molecules (binding to  $\text{SO}_3^-$  group of SDS by hydrogen bond).  
416 Tocopherol (AH) can regenerate  $\text{Fe}^{3+}$  into  $\text{Fe}^{2+}$  (Equation 13). Ferrous ions are then available  
417 to induce more oxidation near the interface.



419 Iron complexation and transfer far from the interface can inhibit lipid oxidation.  
420 However, in the case, complexed iron (II) was near the interface. With a positively charged  
421 interface, tocopherol is more preserved and can react as a radical scavenger (Fukuzawa et al.,  
422 1988; Kristinova et al., 2014).

423 CD and TBARS values followed the same trend at pH 2.5 and 7.2. The oxidative stability  
424 can be ranked in descending order: CTAB > Tween20 > SDS. However, at pH 2.5, the CD  
425 and TBARS values were generally higher than those at pH 7.2. For instance, the CD and  
426 TBARS values of emulsion with SDS emulsifier were respectively 3 and 10 times higher at  
427 acidic pH. As for Tween20 emulsions, the TBARS values present lag phases at pH 7.2  
428 (Figure 4b), in contrast, it increased immediately at pH 2.5 (Figure 4a). Similar trends were  
429 seen for CTAB emulsions: TBARS values were approx. two times higher at lower pH value. At  
430 pH 2.5, citrate was mostly protonated (81%  $\text{CitH}_3$ ), which lead to low iron complexation  
431 (Figure 3). Thus, iron could be mainly present as free ions. Iron can then rapidly migrate to  
432 the oil-water interface and increase the oxidation level. When the interface is negatively  
433 charged (SDS emulsifier) the phenomena are more important. At higher pH, citrate ( $\text{HCit}^{2-}$  &

434 Cit<sup>3</sup>) can complex iron, and by this performs a protective role, oxidation is less important.  
435 However, iron is not fully complexed, and therefore oxidation is not totally stopped. Identical  
436 results were obtained for corn oil-in-water emulsion (Cho et al., 2003).

#### 437 **4. Conclusion**

438 Iron (endogenous or exogenous) can significantly accelerate the lipid oxidation in  
439 oil-in-water emulsions. The iron-oxygen interactions constitute the first step of lipid  
440 oxidation. Hence, an absolute reduction of oxygen could limit lipid oxidation even with iron  
441 presence. Such a solution is not practical nor economical for food industries. Conversely, the  
442 buffer and emulsifier choice can control the oxidation-initiation in emulsions. Buffers chelate  
443 iron ions, and in this way impact its position and prooxidant potential. Factors like pH  
444 (protonation of chelator; pKa values), chelator's affinity to Fe (II) (Binding constants;  $\log\beta$ ),  
445 and the final structure of the complex (number of free coordination sites) influence its  
446 stability and catalytic activity. When the complex structure promotes the iron-oxidation,  
447 oxidation initiation by this complex is retarded. In addition, the buffer-iron complexes allow  
448 iron migration near the positively charged interface, overcoming the repulsive forces.  
449 Therefore, the interface charge has a critical impact on lipid oxidation. Negatively charged  
450 interface increases the rate of oxidation by attracting free and chelated iron ions. Besides,  
451  $\alpha$ -tocopherol near this interface is closer to iron ions which promote its oxidation and Fe (II)  
452 regeneration. Consequently, controlling iron ions interactions with buffers and emulsifiers  
453 could help to limit omega-3 LC-PUFA oxidation in food and drinks.

#### 454 **Acknowledgements**

455 The authors gratefully acknowledge our partner Cargill, the "Fonds Européen de  
456 Développement Régional" (FEDER), and the Regional Council of Bourgogne-Franche-

457 Comté, for their financial support. The authors would like thanking all people who helped in  
458 the experimental work, especially Miss Hoang Phuong Ha.

459 **Conflict of interest**

460 The authors declare that there is no conflict of interest.

461 **References**

- 462 Albert, B. B., Cameron-Smith, D., Hofman, P. L., & Cutfield, W. S. (2013). Oxidation of  
463 Marine Omega-3 Supplements and Human Health. *BioMed Research International*,  
464 2013, 1–8. <https://doi.org/10.1155/2013/464921>
- 465 Cano-Sarmiento, C., Téllez-Medina, D. I., Viveros-Contreras, R., Cornejo-Mazón, M.,  
466 Figueroa-Hernández, C. Y., García-Armenta, E., Alamilla-Beltrán, L., García, H. S.,  
467 & Gutiérrez-López, G. F. (2018). Zeta Potential of Food Matrices. *Food Engineering*  
468 *Reviews*, 10(3), 113–138. <https://doi.org/10.1007/s12393-018-9176-z>
- 469 Cargill. (2014). *Study shows consumers want more omega-3 | Cargill*.  
470 <https://www.cargill.com/news/releases/2014/NA31701258.jsp>
- 471 Cheng, Z., & Li, Y. (2007). What Is Responsible for the Initiating Chemistry of Iron-  
472 Mediated Lipid Peroxidation: An Update. *Chemical Reviews*, 107(3), 748–766.  
473 <https://doi.org/10.1021/cr040077w>
- 474 Cho, Y.-J., Alamed, J., McClements, D. j., & Decker, E. a. (2003). Ability of Chelators to  
475 Alter the Physical Location and Prooxidant Activity of Iron in Oil-in-Water  
476 Emulsions. *Journal of Food Science*, 68(6), 1952–1957.  
477 <https://doi.org/10.1111/j.1365-2621.2003.tb07000.x>
- 478 Codex Alimentarius Commission, FAO, WHO. (2017, Adopted in). *Standard for fish oils*,  
479 *CXS 329-2017*. <http://www.fao.org/fao-who-codexalimentarius>
- 480 Daoud, S., Bou-maroun, E., Dujourdy, L., Waschatko, G., Billecke, N., & Cayot, P. (2019).  
481 Fast and direct analysis of oxidation levels of oil-in-water emulsions using ATR-

482 FTIR. *Food Chemistry*, 293, 307–314.  
483 <https://doi.org/10.1016/j.foodchem.2019.05.005>

484 EFSA. (2014). Scientific Opinion on the substantiation of a health claim related to DHA and  
485 contribution to normal brain development pursuant to Article 14 of Regulation (EC)  
486 No 1924/2006. *EFSA Journal*, 12(10), 3840. <https://doi.org/10.2903/j.efsa.2014.3840>

487 Engelmann, M. D. (2003). Variability of the Fenton reaction characteristics of the EDTA,  
488 DTPA, and citrate complexes of iron. *BioMetals*, 16(4), 519–527.  
489 <https://doi.org/10.1023/A:1023480617038>

490 FAO/WHO. (2008, November 10). WHO | Joint FAO/WHO Expert Consultation on Fats and  
491 Fatty Acids in Human Nutrition (10 - 14 November 2008, WHO, Geneva). *WHO*.  
492 [https://www.who.int/nutrition/topics/FFA\\_interim\\_recommendations/en/](https://www.who.int/nutrition/topics/FFA_interim_recommendations/en/)

493 Ferreira, C. M. H., Pinto, I. S. S., Soares, E. V., & Soares, H. M. V. M. (2015). (Un)suitability  
494 of the use of pH buffers in biological, biochemical and environmental studies and their  
495 interaction with metal ions – a review. *RSC Advances*, 5(39), 30989–31003.  
496 <https://doi.org/10.1039/C4RA15453C>

497 Francis, A. J., & Dodge, C. J. (1993). Influence of Complex Structure on the Biodegradation  
498 of Iron-Citrate Complexes. *Applied and Environmental Microbiology*, 59(1), 109–113.  
499 <https://doi.org/10.1128/AEM.59.1.109-113.1993>

500 Frankel, E. N. (2015). *Lipid Oxidation* (Second edition). Woodhead Publishing.

501 Fukuzawa, K. (2008). Dynamics of lipid peroxidation and antioxidion of alpha-tocopherol in  
502 membranes. *Journal of Nutritional Science and Vitaminology*, 54(4), 273–285.

503 Fukuzawa, K., & Fujii, T. (1992). Peroxide dependent and independent lipid peroxidation:  
504 Site-specific mechanisms of initiation by chelated iron and inhibition by  $\alpha$ -tocopherol.  
505 *Lipids*, 27(3), 227–233. <https://doi.org/10.1007/BF02536183>

506 Fukuzawa, K., Kishikawa, K., Tadokoro, T., Tokumura, A., Tsukatani, H., & Gebicki, J. M.  
507 (1988). The effects of  $\alpha$ -tocopherol on site-specific lipid peroxidation induced by iron  
508 in charged micelles. *Archives of Biochemistry and Biophysics*, 260(1), 153–160.  
509 [https://doi.org/10.1016/0003-9861\(88\)90436-5](https://doi.org/10.1016/0003-9861(88)90436-5)

510 Gliszczyńska-Świąło, A., & Sikorska, E. (2004). Simple reversed-phase liquid  
511 chromatography method for determination of tocopherols in edible plant oils. *Journal*  
512 *of Chromatography A*, 1048(2), 195–198.  
513 <https://doi.org/10.1016/j.chroma.2004.07.051>

514 He, K. (2009). Fish, Long-Chain Omega-3 Polyunsaturated Fatty Acids and Prevention of  
515 Cardiovascular Disease—Eat Fish or Take Fish Oil Supplement? *Progress in*  
516 *Cardiovascular Diseases*, 52(2), 95–114. <https://doi.org/10.1016/j.pcad.2009.06.003>

517 Hoan, P. T., & Son, T. K. (2018). Tra Catfish Oil Production: Phospholipid Removal Using  
518 Citric Acid and Bleaching Using Activated Carbon. *2018 4th International*  
519 *Conference on Green Technology and Sustainable Development (GTSD)*, 528–532.  
520 <https://doi.org/10.1109/GTSD.2018.8595528>

521 Königsberger, L.-C., Königsberger, E., May, P. M., & Hefter, G. T. (2000). Complexation of  
522 iron(III) and iron(II) by citrate. Implications for iron speciation in blood plasma.  
523 *Journal of Inorganic Biochemistry*, 78(3), 175–184. [https://doi.org/10.1016/S0162-](https://doi.org/10.1016/S0162-0134(99)00222-6)  
524 [0134\(99\)00222-6](https://doi.org/10.1016/S0162-0134(99)00222-6)

525 Kristinova, V., Aaneby, J., Mozuraityte, R., Storrø, I., & Rustad, T. (2014). The effect of  
526 dietary antioxidants on iron-mediated lipid peroxidation in marine emulsions studied  
527 by measurement of dissolved oxygen consumption. *European Journal of Lipid Science*  
528 *and Technology*, 116(7), 857–871. <https://doi.org/10.1002/ejlt.201400011>

529 Laguerre, M., Bily, A., Roller, M., & Birtić, S. (2017). Mass Transport Phenomena in Lipid  
530 Oxidation and Antioxidation. *Annual Review of Food Science and Technology*, 8(1),  
531 391–411. <https://doi.org/10.1146/annurev-food-030216-025812>

532 Lee, Y.-M., Hong, S., Morimoto, Y., Shin, W., Fukuzumi, S., & Nam, W. (2010). Dioxygen  
533 Activation by a Non-Heme Iron(II) Complex: Formation of an Iron(IV)–Oxo  
534 Complex via C–H Activation by a Putative Iron(III)–Superoxo Species. *Journal of the  
535 American Chemical Society*, 132(31), 10668–10670.  
536 <https://doi.org/10.1021/ja103903c>

537 Let, M. B., Jacobsen, C., Frankel, E. N., & Meyer, A. S. (2003). Oxidative flavour  
538 deterioration of fish oil enriched milk. *European Journal of Lipid Science and  
539 Technology*, 105(9), 518–528. <https://doi.org/10.1002/ejlt.200300821>

540 Liao, H., Zhu, M., & Chen, Y. (2020). 4-Hydroxy-2-nonenal in food products: A review of  
541 the toxicity, occurrence, mitigation strategies and analysis methods. *Trends in Food  
542 Science & Technology*, 96, 188–198. <https://doi.org/10.1016/j.tifs.2019.12.011>

543 Liu, J., Guo, Y., Li, X., Si, T., McClements, D. J., & Ma, C. (2019). Effects of Chelating  
544 Agents and Salts on Interfacial Properties and Lipid Oxidation in Oil-in-Water  
545 Emulsions. *Journal of Agricultural and Food Chemistry*, acs.jafc.8b05867.  
546 <https://doi.org/10.1021/acs.jafc.8b05867>

547 Long, E. K., & Picklo, M. J. (2010). Trans-4-hydroxy-2-hexenal, a product of n-3 fatty acid  
548 peroxidation: Make some room HNE.... *Free Radical Biology and Medicine*, 49(1),  
549 1–8. <https://doi.org/10.1016/j.freeradbiomed.2010.03.015>

550 Mao, Y., Pham, A. N., Rose, A. L., & Waite, T. D. (2011). Influence of phosphate on the  
551 oxidation kinetics of nanomolar Fe(II) in aqueous solution at circumneutral pH.  
552 *Geochimica et Cosmochimica Acta*, 75(16), 4601–4610.  
553 <https://doi.org/10.1016/j.gca.2011.05.031>



554 Martínez-Navarrete, N., Camacho, M. M., Martínez-Lahuerta, J., Martínez-Monzó, J., & Fito,  
555 P. (2002). Iron deficiency and iron fortified foods—a review. *Food Research*  
556 *International*, 35(2), 225–231. [https://doi.org/10.1016/S0963-9969\(01\)00189-2](https://doi.org/10.1016/S0963-9969(01)00189-2)

557 McDonald, R. E., & Hultin, H. O. (1987). Some Characteristics of the Enzymic Lipid  
558 Peroxidation System in the Microsomal Fraction of Flounder Skeletal Muscle. *Journal*  
559 *of Food Science*, 52(1), 15–21. <https://doi.org/10.1111/j.1365-2621.1987.tb13964.x>

560 Mei, L., McClements, D. J., Wu, J., & Decker, E. A. (1998). Iron-catalyzed lipid oxidation in  
561 emulsion as affected by surfactant, pH and NaCl. *Food Chemistry*, 61(3), 307–312.  
562 [https://doi.org/10.1016/S0308-8146\(97\)00058-7](https://doi.org/10.1016/S0308-8146(97)00058-7)

563 Nazir, N., Diana, A., & Sayuti, K. (2017). Physicochemical and Fatty Acid Profile of Fish Oil  
564 from Head of Tuna (*Thunnus albacares*) Extracted from Various Extraction Method.  
565 *International Journal on Advanced Science, Engineering and Information Technology*,  
566 7(2), 709. <https://doi.org/10.18517/ijaseit.7.2.2339>

567 Pham, A. N., & Waite, T. D. (2008). Oxygenation of Fe(II) in the Presence of Citrate in  
568 Aqueous Solutions at pH 6.0–8.0 and 25 °C: Interpretation from an Fe(II)/Citrate  
569 Speciation Perspective. *The Journal of Physical Chemistry A*, 112(4), 643–651.  
570 <https://doi.org/10.1021/jp0772191>

571 Qian, S. Y., & Buettner, G. R. (1999). Iron and dioxygen chemistry is an important route to  
572 initiation of biological free radical oxidations: an electron paramagnetic resonance  
573 spin trapping study. *Free Radical Biology and Medicine*, 26(11), 1447–1456.  
574 [https://doi.org/10.1016/S0891-5849\(99\)00002-7](https://doi.org/10.1016/S0891-5849(99)00002-7)

575 Schaich, K. M. (1992). Metals and lipid oxidation. Contemporary issues. *Lipids*, 27(3), 209–  
576 218. <https://doi.org/10.1007/BF02536181>

577 Seraghni, N., Belattar, S., Mameri, Y., Debbache, N., & Sehili, T. (2012). Fe(III)-Citrate-  
578 Complex-Induced Photooxidation of 3-Methylphenol in Aqueous Solution.

579 *International Journal of Photoenergy*, 2012, 1–10.  
580 <https://doi.org/10.1155/2012/630425>

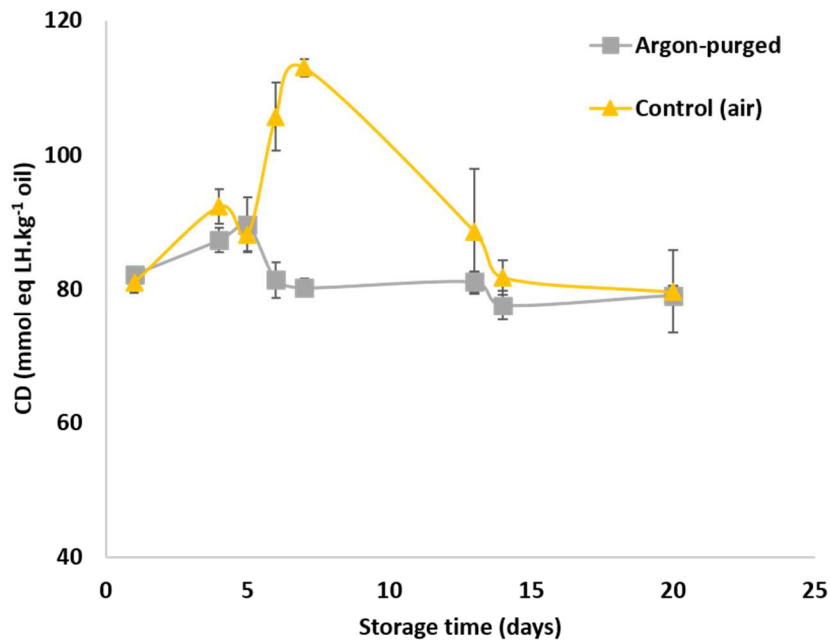
581 Sørensen, A.-D. M., Haahr, A.-M., Becker, E. M., Skibsted, L. H., Bergenståhl, B., Nilsson,  
582 L., & Jacobsen, C. (2008). Interactions between Iron, Phenolic Compounds,  
583 Emulsifiers, and pH in Omega-3-Enriched Oil-in-Water Emulsions. *Journal of*  
584 *Agricultural and Food Chemistry*, 56(5), 1740–1750.  
585 <https://doi.org/10.1021/jf072946z>

586 Stark, K. D., Van Elswyk, M. E., Higgins, M. R., Weatherford, C. A., & Salem, N. (2016).  
587 Global survey of the omega-3 fatty acids, docosahexaenoic acid and eicosapentaenoic  
588 acid in the blood stream of healthy adults. *Progress in Lipid Research*, 63, 132–152.  
589 <https://doi.org/10.1016/j.plipres.2016.05.001>

590 Suseno, S. H., Saraswati, Hayati, S., & Izaki, A. F. (2014). Fatty Acid Composition of Some  
591 Potential Fish Oil from Production Centers in Indonesia. *Oriental Journal of*  
592 *Chemistry*, 30(3), 975–980.

593 Wang, L., Fan, H., He, J., Wang, L., Tian, Z., & Wang, C. (2018). Protective effects of  
594 omega-3 fatty acids against Alzheimer’s disease in rat brain endothelial cells. *Brain*  
595 *and Behavior*, 8(11). <https://doi.org/10.1002/brb3.1037>

596 Yin, D., Lingnert, H., Ekstrand, B., & Brunk, U. T. (1992). Fenton reagents may not initiate  
597 lipid peroxidation in an emulsified linoleic acid model system. *Free Radical Biology*  
598 *and Medicine*, 13(5), 543–556. [https://doi.org/10.1016/0891-5849\(92\)90149-B](https://doi.org/10.1016/0891-5849(92)90149-B)  
599

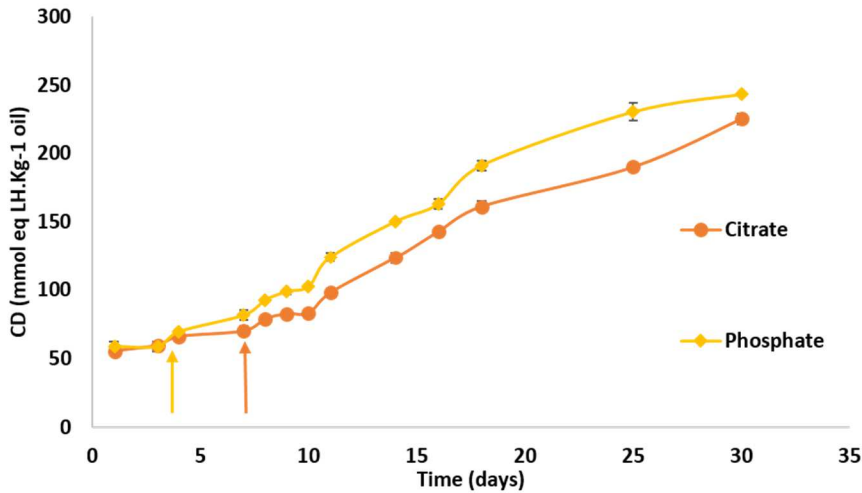


1

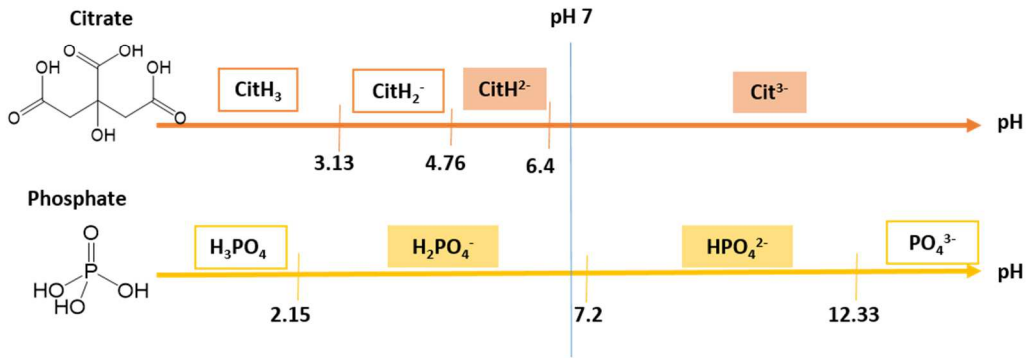
2 Figure 1. Lipid oxidation as measured by conjugated dienes (CD mmol eq peroxide.Kg<sup>-1</sup> of oil)  
 3 for 20% (v/v) tuna oil-in-water emulsions with citrate buffer (1 mM) and iron (II) (0.1 mM).  
 4 Two conditions were studied: (▲) under control atmosphere, air (dioxygen solubilized in the  
 5 emulsion) and (■) after purging with argon (hypoxic condition). Samples were kept in dark at  
 6 30 °C. Data are means of three repetitions. Error bars represent standard deviations

7

a) Oxidation variation depending on buffer choice



b) Iron complexation by buffer depending on pH and pKa

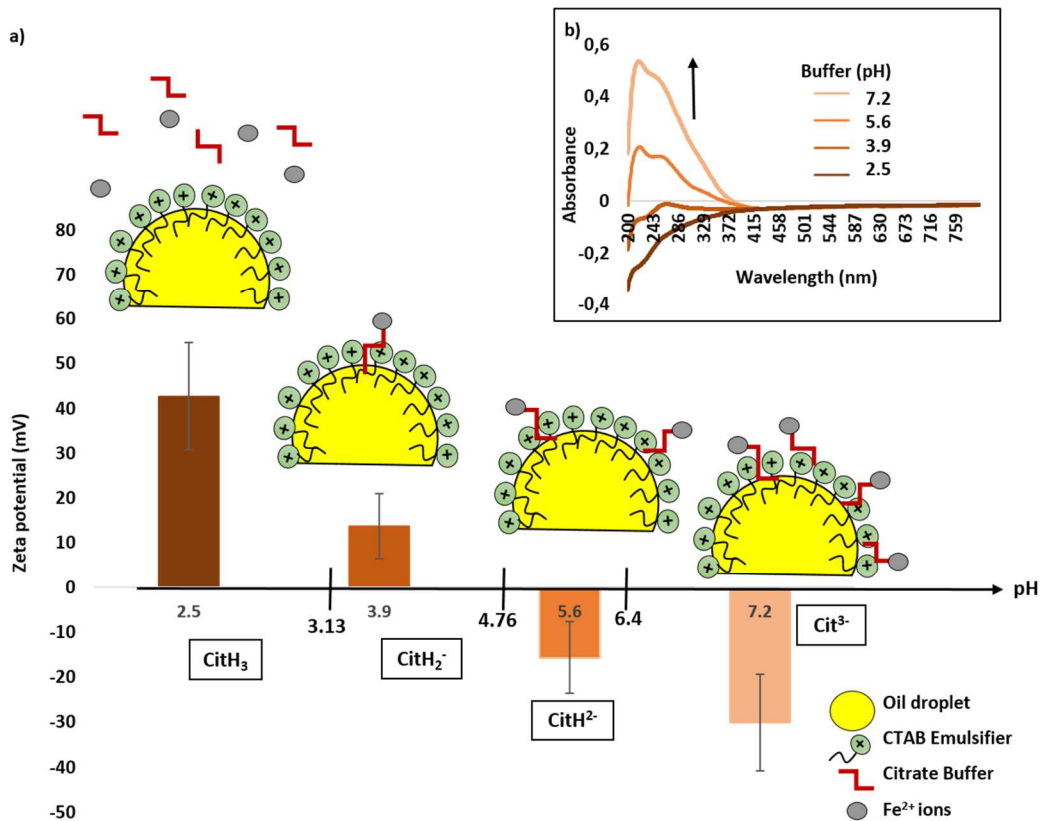


8

9 Figure 2. Buffer influence on iron-induced lipid oxidation: (a) Variations of CD value (mmol  
 10 eq peroxide.Kg<sup>-1</sup> oil) of emulsions (20% v/v oil) oxidized with 0.1 mM of iron and kept in dark  
 11 at 30 °C. Different buffers (1 mM) were used: (●) citrate and (◇) phosphate. Data shown as  
 12 means of three replicates and the error bars represent the standard deviation (sometimes laying  
 13 within the points). Arrows indicate the induction times. (b) Distribution of buffer species  
 14 depending on its pKa values. The pH of all the emulsions was set at 7. Species highlighted are  
 15 theoretically the most abundant at pH 7

16

17



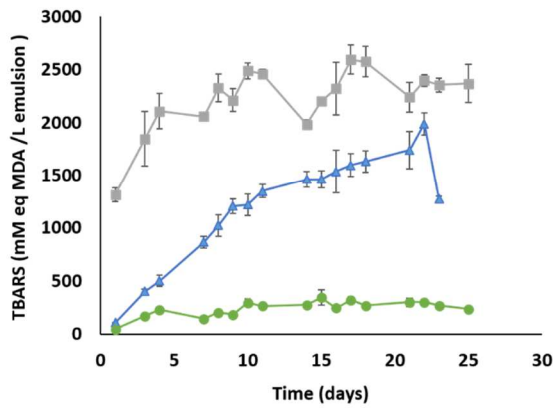
18

19 Figure 3. Impact of the pH level: (a) Variations of zeta potential (mV) of oil-in-water emulsions  
 20 prepared using the citrate buffer (1 mM) at different pH level (2.5, 3.9, 5.6 and 7.2) and a  
 21 simplified proposed design for the oil-water interface at different pH (iron ions complexation  
 22 by citrate buffer and transfer to the interface). Iron was added to a final concentration of  
 23 0.1 mM. Values represent means of 6 repetitions (3 measurements on two different sets). Error  
 24 bars represent standard deviations; (b) Differential UV spectra of iron (0.1 mM) and citrate  
 25 (1 mM) solutions, these solutions were similar but at different pH levels, the peak of iron-citrate  
 26 complex increases when the pH increased

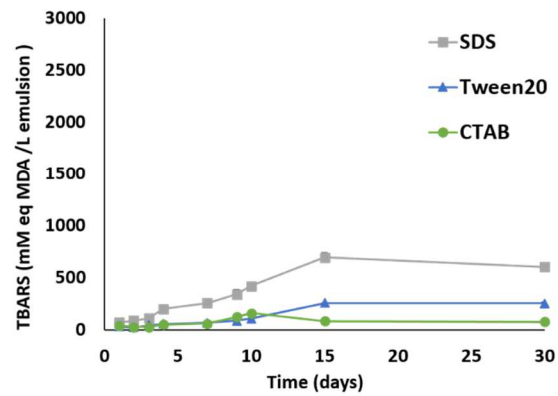
27

28

a) pH 2.5 : 80% CitH<sub>3</sub> / 20% CitH<sub>2</sub><sup>-</sup>



b) pH 7.2 : 14% CitH<sup>2-</sup> / 86% Cit<sup>3-</sup>



29

30 Figure 4. Variations in the oxidation level of oil-in-water emulsion (20 %v/v tuna oil) as  
 31 evaluated by the TBARS value (mM of eq MDA.L<sup>-1</sup> emulsion) at pH 2.5 (a) and pH 7.2 (b). All  
 32 emulsions were prepared with citrate buffer (1 mM) with added iron (II) (0.1 mM), and kept in  
 33 dark at 30 °C. Three different emulsifiers were used: (●) CTAB<sup>+</sup> (cetyltrimethylammonium  
 34 bromide, positively charged), (▲) Tween<sup>0</sup> (Tween20, neutral) and (■) SDS<sup>-</sup> (sodium  
 35 dodecylsulfate, negatively charged). Data represent means of three repetitions and error bars  
 36 are standard deviations

- 1 Table 1. Characterization of tuna oil used in this study: fatty acids composition, tocopherol
- 2 and iron contents

<b>Fatty acids</b>	<b>Mean % wt.</b>	<b>3</b>
14:0	3.43 ± 0.31	
15:0	0.87 ± 0.08	
16:0	19.51 ± 0.53	
17:0	1.17 ± 0.06	
18:0	6.12 ± 0.17	
19:0	0.25 ± 0.04	
<b>Total SFA</b>	<b>31.35</b>	
16:1 (n-7)	5.22 ± 0.38	
17:1	0.66 ± 0.04	
18:1 (n-9)	18.82 ± 0.68	
20:1	1.82 ± 0.15	
22:1	0.28 ± 0.04	
<b>Total MUFA</b>	<b>26.79</b>	
16:2	1.32 ± 0.18	
18:2 (n-6) (LA)	1.92 ± 0.08	
20:4 (n-6)	1.84 ± 0.43	
20:5 (n-3)(EPA)	8.92 ± 0.91	
22:5	1.92 ± 0.07	
22:6 (n-3) (DHA)	25.26 ± 0.63	
<b>Total PUFA</b>	<b>41.17</b>	
<b>DHA/EPA</b>	<b>2.83</b>	
<b>Total n-3</b>	<b>34.18</b>	
<b>Total n-6</b>	<b>3.76</b>	
<b>Iron (mg.Kg<sup>-1</sup> oil)</b>	<b>0.71 ± 0.35</b>	
<b>α-tocopherol (mg.Kg<sup>-1</sup> oil)</b>	<b>1282 ± 209</b>	